Interstellar Optics

C.R. Gwinn¹, M.C. Britton^{1,2}, J.E. Reynolds³, D.L. Jauncey³, E.A. King³, P. M. McCulloch⁴, J.E.J. Lovell^{4,5} & R.A. Preston⁶

- ¹ Physics Department, University of California, Santa Barbara, California, 93106, USA
- 2 Present address: School of Physics, University of Melbourne, Parkville 3052, Victoria, Australia
- ³ Australia Telescope National Facility, Epping, New South Wales, 2121, Australia
- ⁴ Physics Department, University of Tasmania, Hobart, 7001, Tasmania, Australia
- ⁵ Present address: Institute of Space and Astronautical Science, 3-1-1 Yoshinodai, Sagamihara, Kanagawa 229, Japan
- 6 Jet Propulsion Laboratory, California Institute of Technology, Pasadena, California, 91109, USA

ABSTRACT

We discuss the effects of finite source size on the diffraction pattern produced by scattering in a thin screen, particularly as applied to radio-wave scattering. by density fluctuations in the interstellar plasma. Using the stationary phase approximation, we express the Kirchoff integral for the diffracted electric field as a phasor sum, and show that source structure introduces correlations between such sums, combined to form intensity or interferometric visibility. We obtain expressions for the probability distribution functions of intensity of a source of finite size, and of interferometric visibility on a baseline shorter than the scale of the diffraction pattern. We also present expressions for the first and second moments of intensity and visibility, for arbitrary source structure, and for sources with Gaussian distribution of intensity. We also present results for sources that radiate Gaussian beams, possibly with imperfect spatial coherence. With these results, observations of the diffracted electric field yield information on the structure of the scattered source, with angular resolution corresponding to the diffraction limit of the scattering disk. These results are of interest for studies of pulsars and other extremely compact radio sources.

Subject headings: scattering – techniques: interferometric – telescopes – pulsars: general

1. Introduction

This paper discusses techniques to infer the structure of astrophysical radio sources scattered by the interstellar plasma, through a statistical analysis of their scattered radio emission. These techniques rest on the fact that, like other optical systems, radio-wave scattering interstellar plasma produces a diffraction pattern in the plane of the observer that is the convolution of the response to a point source, with an image of the source (Goodman 1968, Cornwell et al. 1989). These techniques are to be distinguished from the many, often highly successful techniques that remove effects of scattering to restore "ideal" instrumental performance (see, for example, Pearson & Readhead 1984, Goodman 1985, Beckers 1993, Roggemann, Welsh, & Fugate 1997). The scattering material is part of our instrument: it sets the angular resolution. This angular resolution is that of an aperture with diameter equal to the "scattering disk": the region from which the observer receives scattered radiation. Effects of radio-wave scattering in the interstellar plasma increase the potential diffraction-limited resolution of Earth-based radio observations to nanoarcseconds.

A number of studies have addressed the problem of inferring source structure from the statistics of scintillation. Salpeter (1967) and Cohen, Gundermann, & Harris (1967) derive a relationship between source size and the depth of modulation of scintillation, which we discuss in § 6.2 below. Cohen et al. used this relationship to set limits on the intrinsic sizes of extragalactic sources from their scintillation in the solar wind. This technique has become standard, particularly for measurements of the size of radio sources scatter-broadened by the interstellar plasma, from their scintillation in the solar wind (Hewish, Readhead, & Duffett-Smith 1974, Armstrong & Coles 1978, Rao & Ananthakrishnan 1984, Hajivassiliou 1992).

Introducing a complementary technique, Backer (1975) and Cordes, Weisberg, & Boriakoff (1983) set upper limits on displacement of pulsars' emission regions over the

course of their pulses, by comparing the scintillation patterns at different times throughout the pulse. Wolszczan & Cordes (1987) and Wolszczan, Bartlett, & Cordes (1988) observed occurrences of periodic "fringes" in the scintillation pattern of pulsars B1237+25 and B1133+16, and interpret them as the result of interference between 2 widely-separated paths through the interstellar plasma. They observe displacement of the fringes over the pulse, which they interpret as motion of the emission region. Smirnova, Shishov, & Malofeev (1996) searched for such displacement at an observing frequency of 102.7 MHz, and observe changes of the diffraction patterns over the pulses of pulsars B0834+06, B1133+16, B1237+25, and B1919+21.

Cornwell, Anantharamaiah, & Narayan (1989) adopted a more general approach. They noted that the diffraction pattern in the plane of the observer is the convolution of an image of the source with the response of the optical system to a point source – the "point spread function". (Of course, for scattering by a random medium, the point spread function is not condensed in a central region, as it commonly is for imperfect optical systems.) For scattering by a thin screen, the point spread function is the Fourier transform of the geometric plus scattering phase. Cornwell et al. noted that a Fourier transform technique used for calibrating imperfections in the reflecting surfaces of antennas to obtain diffraction-limited images (Cornwell & Napier 1988) could also be used to image sources scattered by the solar wind or the interstellar medium; they noted that this technique requires impractically large filled apertures. Cornwell & Narayan (1993) suggested techniques that involve comparison of signals among only 4 to 6 antennas. Because most radiotelescope arrays are not only poorly filled, but are dominated by baselines from a single large aperture to a number of small ones, we reduce the problem to that of 2 antennas observing a scintillating source.

Fluctuations in the density of free electrons in the interstellar plasma produce variations

in the index of refraction. A pointlike source observed through such a medium produces a random diffraction pattern in the plane of the observer. The scattering is said to be "strong" if phase differences among different paths are greater than 2π . At wavelengths longer than a few cm, the scattering of pulsars by fluctuations in interstellar electron density is usually extremely strong. In strong scattering both the amplitude and phase of the diffracted electric field vary with location in the observer plane: the diffraction pattern is complex. The spatial scale of the diffraction pattern at the observer is the linear resolution of the scattering disk, treated as a lens: about λ/θ , where λ is the observing wavelength and θ is the angular size of the scattering disk. The observer sees the source scintillate on a timescale $t_{\rm ISS} = \lambda/\theta V_{\perp}$ as he moves through the diffraction pattern with transverse velocity V_{\perp} . The diffraction pattern also changes with observing frequency, with characteristic bandwidth $\Delta \nu_d$, because phase differences among the lines of sight from the scattering disk to the observer's location change with frequency. Observations of the diffraction pattern thus require time averaging of less than $t_{\rm ISS}$ and frequency averaging of less than $\Delta \nu_d$. Such observations are said to be in the speckle limit of interstellar scattering (Desai et al. 1992).

In this paper we explore the effects of finite source size on several observable quantities that measure interstellar scattering. In § 2 we introduce the thin-screen approximation for scattering and the Kirchoff integral for the electric field. We introduce the stationary phase approximation, and express the Kirchoff integral as a phasor sum. We point out that this is essentially the "high-frequency approximation" of Rumsey (1975). We then apply this expression to several scattering observables. In § 3 we present expressions for intensity and interferometric visibility for a point source and extended, spatially-incoherent sources. In § 4 we calculate the average interferometric visibility for a point source, and for small extended sources. In § 5 we find the probability distribution functions for the intensity of a small extended source, and for the interferometric visibility on a short baseline. In § 6 we present expressions for the decorrelation bandwidth of intensity and of the interferometric

visibility, for general source structure and for elliptical Gaussian distributions of intensity. In § 7 we generalize these results to a simple model of a fully or partially spatially-coherent source that radiates a Gaussian beam. In § 8 we summarize the results.

2. Kirchoff Diffraction and the Stationary Phase Approximation

2.1. Kirchoff diffraction

Kirchoff diffraction relates the electric field at the source to that in the plane of the observer (Born & Wolf 1980, Goodman 1985). The electric field in the plane of the observer $E(\mathbf{p})$ is calculated as the double integral of the electric field over all points \mathbf{s} on the source and over all points \mathbf{x} on the scattering screen.

$$E(\mathbf{p}) = \int_{\text{screen}} d\mathbf{x} \frac{e^{ik|\mathbf{d}|}}{|\mathbf{d}|} e^{i\Phi(\mathbf{x})} \int_{\text{source}} d\mathbf{s} \frac{e^{ik|\mathbf{r}|}}{|\mathbf{r}|} E(\mathbf{s}). \tag{1}$$

Here $\mathbf{r} = \mathbf{R} + (\mathbf{x} - \mathbf{s})$ and $\mathbf{d} = \mathbf{D} + (\mathbf{p} - \mathbf{x})$, where \mathbf{R} is the separation of source plane and scattering screen and \mathbf{D} is the separation of screen and observer plane. Figure 1 shows the geometry. The phase introduced by the screen is $\Phi(\mathbf{x})$, and the wavenumber is $k = 2\pi/\lambda$. In the paraxial approximation, the deflections \mathbf{s} , \mathbf{x} , and \mathbf{p} are assumed small with respect to \mathbf{R} and \mathbf{D} , and the integrals can be recast as a double Fourier transform, with multiplication by a "transmission function" between the two transforms (Cornwell & Napier 1988, Cornwell et al. 1989):

$$E(\mathbf{p}) = \frac{e^{iC}}{RD} \int_{\text{screen}} d\mathbf{x} \, e^{-i(k/D)\mathbf{p} \cdot \mathbf{x}} \, e^{i\phi(\mathbf{x})} \int_{\text{source}} d\mathbf{s} \, e^{-i(k/R)\mathbf{s} \cdot \mathbf{x}} E(\mathbf{s}). \tag{2}$$

The phase of the transmission function, $\phi(\mathbf{x}) = \{\Phi(\mathbf{x}) + k[\frac{1}{2D} + \frac{1}{2R}]x^2\}$, is the screen phase $\Phi(\mathbf{x})$ plus the parabolic part of the geometric phase, $k[\frac{1}{2D} + \frac{1}{2R}]x^2$. The geometric phase defines the Fresnel zones at the scattering disk (Jackson 1975). The constant phase C absorbs large, arbitrary phases proportional to the distances D and R. We absorb the

quadratic phase $ks^2/2D$ into the phase of the source, which varies quickly with location, particularly for an incoherent source, as discussed in § 3.2 below. For interstellar scattering, quadratic phase in the observer plane, $kp^2/2R$, varies over a scale of more than 10^6 km, longer than any interferometer baseline; we thus ignore it. This phase could also be removed instrumentally, if baselines long enough to detect it were available.

A traditional lens works by arranging the screen phase $\Phi(\mathbf{x})$ to precisely cancel the geometric phase, so that the double Fourier transform results in an image of the source in the observer plane (Goodman 1968). In interstellar scattering the screen phase is random. If the statistics of the screen are stationary in \mathbf{x} , the phase structure function $D_{\phi}(\mathbf{b}) = \langle (\Phi(\mathbf{x} + \mathbf{b}) - \Phi(\mathbf{x}))^2 \rangle$ characterizes $\Phi(\mathbf{x})$. Here the angular brackets $\langle ... \rangle$ indicate averaging over an ensemble of screens with identical statistical properties. For power-law spectra of density fluctuations, perhaps resulting from a turbulent cascade, $D_{\phi}(\mathbf{b})$ takes a power-law form over some range of separation \mathbf{b} (Rickett 1977, Higdon 1984, Montgomery, Brown, & Matthaeus 1987, Spangler & Gwinn 1990, Goldreich & Sridhar 1995).

As Eq. 2 shows, interstellar scattering acts like an imperfect optical system in that the diffraction pattern in the plane of the observer is the convolution of the diffraction pattern of a point source (the "point spread function") with a magnified image of the source. The magnification factor is M = D/R. If the source is spatially incoherent (as are nearly all terrestrial and astrophysical sources) then the intensity of the diffraction pattern is the convolution of the intensity pattern for a point source with the intensity structure of the source. If the source is spatially coherent (as are laboratory lasers, mirages, and scattering disks treated as sources) then the electric field of the diffraction pattern is the convolution of the electric field for a point source with the electric field of the source (Goodman 1968).

2.2. Stationary phase approximation and application

2.2.1. Points of stationary phase

The stationary phase approximation (Jackson 1975, Born & Wolf 1980) can be useful for the study of strong scattering by a thin screen. This approximation ignores all contributions to the integral over the screen in Eq. 2, except at points where the phase of the integrand has zero derivative with respect to \mathbf{x} . We denote these points of stationary phase $\{\mathbf{x}_i\}$. The approximation is most accurate in the limit where the phase wraps through many turns between these points; contributions from other points average away. This approximation thus ignores all points except those where the gradient of the screen phase precisely cancels that of the geometric phase.

The distribution of points of stationary phase over the screen defines the "scattering disk": the region from which the observer receives radiation. The size of the scattering disk defines θ : $\theta = \sqrt{\langle \mathbf{x}_i^2 \rangle}/D$. Here the angular brackets $\langle ... \rangle$ again indicate averaging over an ensemble of screens with identical statistical properties. Sometimes the refractive scale, $r_R = \theta D$, is used to characterize the scattering disk.

The Fresnel scale, $r_F = \left(k\left[\frac{1}{2D} + \frac{1}{2R}\right]\right)^{-1/2}$, parametrizes the variation of geometric phase. The length r_d for which $D_\phi(r_d) = 1$ characterizes the variation of screen phase. In strong scattering $r_d << r_F << r_R$: the screen phase varies greatly within each Fresnel zone, and the scattering disk covers many Fresnel zones (Cohen & Cronyn 1974, Narayan & Goodman 1989). Thus we expect many points of stationary phase to contribute to the integral in Eq. 2.

A point of stationary phase \mathbf{x}_i contributes $\exp\{i\phi_i\}/H_i$ to the integral over \mathbf{x} in Eq. 2,

where ϕ_i is the phase of the integrand at \mathbf{x}_i , and H_i gives the sharpness of the extremum:

$$\phi_i = \phi(\mathbf{x}_i), \qquad H_i = \left| \det \left| \frac{\partial^2 \phi}{\partial x_m \partial x_n} \right|_{\mathbf{x}_i} \right|^{1/2}.$$
 (3)

Here m and n take the values ξ and η , denoting the 2 dimensions in the plane of the screen. We define coordinates parallel to these directions: (s_{ξ}, s_{η}) in the source plane, (ξ, η) at the screen, and (p_{ξ}, p_{η}) in the observer plane. The electric field of a strongly-scattered source can thus be written as a phasor sum over the points of stationary phase:

$$E(\mathbf{p}) = \sum_{i} \frac{1}{H_{i}} e^{i\phi_{i}} e^{-i(k/D)\mathbf{p}\cdot\mathbf{x}_{i}} \int_{\text{source}} d\mathbf{s} \, e^{-i(k/R)\mathbf{x}_{i}\cdot\mathbf{s}} \, E(\mathbf{s}). \tag{4}$$

For convenience we absorb the constant factor e^{iC}/RD into the screen phase, and thus into $e^{i\phi_i}$. In Figure 2 we plot $\phi(\mathbf{x})$ and the resulting points of stationary phase for a sample screen.

2.2.2. Phases of stationary phase points

In strong scattering, the screen phase varies much more rapidly than the geometric phases; both vary by many turns across the scattering disk. Thus, the phases of the individual points of stationary phase are distributed evenly in phase, modulo 2π . The correlation of points of stationary phase depends on the statistics of $\Phi(\mathbf{x})$. If, for example, the screen is the sum of many individual phase-shifting "clouds," each with spatial scale a and each responsible for many turns of phase, then the separation of stationary phase points is about a, their phases are uncorrelated, and phases of even the closest points of stationary phase differ by many turns. However, observations of turbulent fluids, measurements of scattering, and theoretical work on plasma turbulence motivate power-law spectra spectra of density variations in the screen (Lee & Jokipii 1976, Cordes, Weisberg & Boriakoff 1985, Gwinn et al. 1988, Goldreich & Sridhar 1995, and references therein). These studies commonly suggest a power-law index near that of Kolmogorov turbulence, The power-law

extends from some maximum outer scale a_0 down to a minimum inner scale a_1 . The points of stationary phase are then separated by about the inner scale. If $r_d \ll a_1$ then the stationary phase approximation holds. However, some evidence indicates that $r_d \sim a_1$, at least for heavily-scattered sources (Spangler & Gwinn 1990, Molnar et al. 1995, Wilkinson et al. 1994), although the effects are quite subtle.

Even in cases where the stationary phase approximation is not valid, the Fresnel integral over the screen can certainly be represented as a phasor sum, and in strong scattering the phases will be distributed evenly over 2π . Rumsey (1975) and Codona et al. (1986) note that in strong scattering, points within a distance r_d of some point \mathbf{x} on the screen are likely to have the same phase, to within about a radian. Points with much greater separations have phase differences of many turns, so that their products can be taken to be uncorrelated. This is the "high-frequency approximation" of Rumsey. In this picture, a single phase and weight can describe the Fresnel integral within such a neighborhood, and the integral becomes sum over neighborhoods. The phase ϕ_i and weight H_i have different interpretations from the stationary-phase approximation, however.

Even within the stationary-phase approximation, points at large separations can have correlated phases because of fluctuations with large spatial scales. However, in strong scattering, the difference in phase is many times 2π , so that the distribution of phase difference, modulo 2π , is uniform. For observations at a single frequency, the phases ϕ_i can thus be regarded as uncorrelated. However, small changes Δk in observing wavenumber k can produce correlated changes in screen phase $\Phi(\mathbf{x})$ over large regions. Codona et al. (1986) investigate these carefully for the correlation function of intensity with frequency and position, and find that the effects are small for localized regions in the observer plane: $\Delta p << \theta D$. Therefore, we assume in this work that the integral over the screen can be approximated by a sum of uncorrelated phasors, as in Eq 4.

2.2.3. Source size, baseline length, and frequency shift

A displacement of source or observer introduces a phase gradient across the screen, and a frequency change introduces a parabolic phase change. In either case, the locations of points of stationary phase shift. However, for small displacements or changes in frequency, the points of stationary phase do not move far. This results from the fact that in strong scattering, the screen phase $\Phi(\mathbf{x})$ varies much more rapidly than the parabolic geometric phase $k\left[\frac{1}{2D} + \frac{1}{2R}\right]x^2$ (Cohen & Cronyn 1974), so that the extrema of phase are sharp compared with the smooth phase gradients introduced by small changes in geometrical parameters. For a displacement of the source Δs , the phase gradient is approximately $(k\Delta s/R)x$. This gradient shifts the location of a point of stationary phase, by about $\Delta x \sim \Delta s \, r_d^2/r_F^2$. (Here we assume that, approximately, $r_F^2 \sim R/k \sim D/k$.) A similar expression holds for shift in position of the observer Δp . In strong scattering, $r_d \ll r_F$, and the phase and strength of the point of stationary phase remain nearly unchanged for small displacements at the source. Similarly, for a change in wavenumber Δk , the shift of a point of stationary phase is $\Delta x \sim \frac{\Delta k}{k} r_d$, where we use the fact that for a "typical" point of stationary phase, $x \approx \theta D = r_F^2/r_d$. For small changes in observing frequency, $\Delta k \ll k$, and the phase and strength of the point of stationary phase again remain nearly unchanged.

The goal of our theoretical studies is to provide comparisons for observations. Such observations measure moments of the electric field $E(\mathbf{p})$ in the observer plane. Little information is gained from a single observation of the scintillation pattern. Statistical averages, perferably of many realizations of particular screens, are most useful for comparison of theory and observation. We consider such statistical averages in the remainder of this paper.

3. Intensity and Interferometric Visibility

3.1. Point source

The simplest observable quantity is the intensity, the square modulus of electric field.

$$I = \langle EE^* \rangle_{1/B} \tag{5}$$

Here the subscripted angular brackets $\langle ... \rangle_{1/B}$ indicate that we average the electric field over a time interval much greater than the reciprocal of the observing bandwidth, but not over more than a single set of points of stationary phase. Such a set corresponds to a single realization of the scattering screen, or a single scintillation timescale and bandwidth. For a point source, $E(\mathbf{s}) = E_0 \, \delta(\mathbf{s})$, and Eq. 4 shows that the electric field E is a random phasor sum, with statistics of a random walk. The intensity of a point source is:

$$I = \left(\sum_{i} \frac{e^{i\phi_{i}}}{H_{i}}\right) \left(\sum_{j} \frac{e^{-i\phi_{j}}}{H_{j}}\right) |E_{0}|^{2} \tag{6}$$

Here, without loss of generality we take $\mathbf{p} = 0$. This equation shows that the intensity is the square modulus of a sum of random phasors, with phases distributed randomly between 0 and 2π .

The correlated flux density, or visibility, measured by interferometry is the product of electric fields at 2 different locations A and B.

$$C_{AB} = \langle E(A)E^*(B)\rangle_{1/B}. \tag{7}$$

Without loss of generality, we assume that station B lies at $\mathbf{p} = 0$ and station A lies at $\mathbf{p} = \mathbf{b}$. For a point source, the visibility C_{AB} is then:

$$C_{AB}(\mathbf{b}) = \left(\sum_{i} \frac{e^{i\phi_{i}}}{H_{i}} e^{-i(k/D)\mathbf{b}\cdot\mathbf{x}_{i}}\right) \left(\sum_{j} \frac{e^{-i\phi_{j}}}{H_{j}}\right). \tag{8}$$

Note that this is precisely the expression for the intensity, except for the factor $e^{-i(k/D)\mathbf{b}\cdot\mathbf{x}_i}$ in the first sum.

3.2. Extended, spatially-incoherent source

For a spatially-incoherent source, the electric field is noiselike at each point on the source and is uncorrelated between different locations s_1 and s_2 :

$$\langle E(\mathbf{s}_1)E^*(\mathbf{s}_2)\rangle_{1/B} = I(\mathbf{s}_1)\,\delta(\mathbf{s}_1 - \mathbf{s}_\eta) \tag{9}$$

Here the subscripted angular brackets $\langle ... \rangle_{1/B}$ again indicate that we average the product of electric fields over a time interval much greater than the reciprocal of the observing bandwidth.

Scattering preserves the spatial coherence of the source (Born & Wolf 1980, Goodman 1985, Cornwell et al. 1989). Using Eqs. 4 and 9, we find the expression for intensity of the scattered source is:

$$I = EE^* = \left(\sum_{i} \frac{e^{i\phi_i}}{H_i} e^{i\phi_i}\right) \left(\sum_{j} \frac{e^{-i\phi_j}}{H_j}\right) \int_{\text{source}} d\mathbf{s} \, I(\mathbf{s}) \, e^{i(k/R)(\mathbf{x}_j - \mathbf{x}_i) \cdot \mathbf{s}}$$
(10)

Without loss of generality we take $\mathbf{p} = 0$. The visibility is:

$$C_{AB}(\mathbf{b}) = \left(\sum_{i} \frac{e^{i\phi_{i}}}{H_{i}} e^{-i(k/D)\mathbf{b}\cdot\mathbf{x}_{i}}\right) \left(\sum_{j} \frac{e^{-i\phi_{j}}}{H_{j}}\right) \int_{\text{source}} d\mathbf{s} \, I(\mathbf{s}) \, e^{i(k/R)(\mathbf{x}_{j} - \mathbf{x}_{i})\cdot\mathbf{s}}$$
(11)

For both intensity and visibility, the nonzero size of the source introduces correlations between sums over i and j: each product is multiplied by a Fourier component of the intensity distribution of the source. Indeed, this Fourier component is simply the interferometric visibility that would be measured on the interferometer baseline $\mathbf{x}_i - \mathbf{x}_j$ between the 2 points of stationary phase. In interstellar scattering, these points can be separated by as much as a few AU.

As a concrete example, appropriate for many simple source structures, consider a source with a circular Gaussian distribution of intensity, with full width at half maximum $\sqrt{8 \ln 2\sigma}$:

$$I(\mathbf{s}) = I_0 \exp\left\{-\frac{1}{2} \frac{s^2}{\sigma^2}\right\}.$$
 (12)

Note that σ is the linear size of the source; $\sigma/(R+D)$ is the angular size as viewed from the observer. The Fourier transform of this distribution is also Gaussian, with standard deviation $k\sigma/R$. The expression for interferometric visibility is then:

$$C_{AB}(\mathbf{b}) = \left(\sum_{i} \frac{e^{i\phi_{i}}}{H_{i}} e^{-i(k/D)\mathbf{b}\cdot\mathbf{x}_{i}}\right) \left(\sum_{j} \frac{e^{-i\phi_{j}}}{H_{j}}\right) e^{\left\{-\frac{1}{2}(k\sigma/R)^{2}|\mathbf{x}_{j}-\mathbf{x}_{i}|^{2}\right\}}$$

$$= \left(\sum_{i} G_{i} e^{-i(k/D)\mathbf{b}\cdot\mathbf{x}_{i}}\right) \left(\sum_{j} G_{j}^{*}\right) e^{(k\sigma/R)^{2}\mathbf{x}_{j}\cdot\mathbf{x}_{i}},$$

$$(13)$$

where the new phasors are

$$G_{i} = \frac{e^{i\phi_{i}}}{H_{i}} e^{-\frac{1}{2}(k\sigma/R)x_{i}^{2}}.$$
(14)

Note that G_i is complex. This expression shows explicitly how an extended source introduces correlations between the sums over i and j in Eq. 11. These correlations decrease the relative weights of terms in the product of sums for which \mathbf{x}_i and \mathbf{x}_j are far apart. This decrease acts to effectively "vignette" the scattering disk: it reduces the effect of points of stationary phase near its periphery, because such points have fewer close neighbors, on the average, than points near the center of the scattering disk. The expression for G_i shows this reduction. The expression for intensity is the same, with $\mathbf{b} = 0$.

4. Second Moments: Average Visibility

4.1. Average visibility for a point source

The normalized average visibility on interferometer baseline **b** is $\bar{V}(\mathbf{b}) = \langle C_{AB}(\mathbf{b}) \rangle / \langle I \rangle$. The angular brackets $\langle ... \rangle$ denote an average over an ensemble of screens with similar statistics. The normalization factor $\langle I \rangle$ is the average intensity; because intensity is the interferometric visibility at zero baseline, $\bar{V}(0) = 1$. Commonly, the average visibility is related to the phase structure function of the screen, $D_{\phi}(\mathbf{x})$, using Eq. 2 (Rumsey 1975, Rickett 1977). This derivation involves the small phase differences between pairs of

points close together on the screen, as quantified by the phase structure function. Here we follow a different approach, based on our assumption that stationary phase points have uncorrelated phases. We later adapt this to sources with finite size.

For a point source, Eq. 8 shows:

$$\bar{V}(\mathbf{b}) = \frac{1}{\langle I \rangle} \langle C_{AB}(\mathbf{b}) \rangle = \frac{1}{\langle I \rangle} \left\langle \sum_{i} \frac{e^{i\phi_{i}}}{H_{i}} e^{-i(k/D)\mathbf{b} \cdot \mathbf{x}_{i}} \sum_{j} \frac{e^{-i\phi_{j}}}{H_{j}} \right\rangle. \tag{15}$$

The angular brackets indicate an average over an ensemble of screens, with the points weighted by $1/H_i^2$. In the product of sums within angular brackets, the phases of the stationary phase points cancel for terms with i = j, so that these terms can contribute to the ensemble average. Following our assumption that the phases of points of stationary phase are uncorrelated, the terms in the product with $i \neq j$ have large, random phases; modulo 2π , they are unformly distributed, and average to 0 over the ensemble.

Thus, we find

$$\bar{V}(\mathbf{b}) = \frac{1}{\langle I \rangle} \left\langle \sum_{i} \frac{1}{H_{i}^{2}} e^{-i(k/D)\mathbf{b} \cdot \mathbf{x}_{i}} \right\rangle. \tag{16}$$

We define $P(\mathbf{x})$ to be the probability over the ensemble of finding a point of stationary phase at \mathbf{x} , weighted by strength $1/H(\mathbf{x})^2$. Then

$$\bar{V}(\mathbf{b}) = \int d\mathbf{x} P(\mathbf{x}) e^{-i(k/D)\mathbf{b}\cdot\mathbf{x}_i}$$
(17)

Note that $P(\mathbf{x})$ is the distribution of intensity for a scattered point source, averaged over an ensemble of scattering screens. The normalized average visibility is simply the Fourier transform of $P(\mathbf{x})$. This agrees well with the simple picture where the observer sees the points of stationary phase as "speckles", distributed over the scattering disk according to the probability density function $P(\mathbf{x})$, with the strength of each point given by $1/H(\mathbf{x})^2$. The interferometer measures one component of the Fourier transform of that source structure. Observations with many baselines, within the speckle limit, can produce an image showing the points of stationary phase (see, for example, Cornwell et al. 1989).

To an excellent approximation, the derivative of screen phase $\partial \Phi/\partial \mathbf{x}$ is drawn from a Gaussian distribution. To a good approximation, the H_i are uncorrelated with $\partial \Phi/\partial \mathbf{x}|_{\mathbf{x}_i}$. In this case, the distribution on the screen of points of stationary phase \mathbf{x}_i is also Gaussian:

$$P(\mathbf{x}) = \frac{1}{2\pi\theta^2 D^2} \exp\left\{-\frac{|\mathbf{x}|^2}{2\theta^2 D^2}\right\}.$$
 (18)

Here θ is the observed angular size of the scattering disk:

$$\theta^2 = \frac{1}{D^2} \langle x_i^2 \rangle. \tag{19}$$

Under the usually excellent approximation that the weights $1/H_i$ are uncorrelated with \mathbf{x}_i , the average in Eq 17 yields for the normalized average visibility of a point source:

$$\ddot{V}(\mathbf{b}) = \frac{1}{\langle I \rangle} \langle C_{AB} \rangle$$

$$= \int d\mathbf{x} P(\mathbf{x}) e^{-i(k/D)\mathbf{b} \cdot \mathbf{x}}$$

$$= \exp \left\{ -\frac{1}{2} (k\theta b)^2 \right\}$$
(20)

Note that \bar{V} must be real. This serves as an alternative definition for θ .

The density fluctuations responsible for interstellar scattering appear to follow a power-law spatial spectrum, perhaps over several orders of magnitude in spatial wavenumber. For a power-law spectrum of fluctuations of $\Phi(\mathbf{x})$, the distribution on the scattering screen of points of stationary phase \mathbf{x}_i is Gaussian, but H_i is weakly correlated with $\partial \Phi/\partial \mathbf{x}|_{\mathbf{x}_i}$, and so with $|\mathbf{x}_i|$. This leads to a slight departure of the average visibility from a Gaussian distribution. This departure has been predicted theoretically (Rumsey 1975, Rickett 1977) and is observed for some sources (Gwinn et al. 1988, Gwinn, Moran, & Reid 1990, Moran et al. 1990, Wilkinson et al. 1994, Molnar et al. 1995). For studies of effects of source structure on scattering observables, Eq. 18 is an excellent approximation.

In general, particularly for scattering in the magnetized interstellar plasma, the scattering is anisotropic, so that $\theta_{\xi} \neq \theta_{\eta}$ (Wilkinson et al. 1994, Goldreich & Sridhar

1995, Desai, Gwinn, & Diamond 1995, Trotter, Moran, & Rodriguez 1998). In practice, it is often most convenient to scale coordinates in the observer and source planes to account for this anisotropy.

4.2. Average visibility for an incoherent source

If the source has nonzero size, but is small enough that the points of stationary phase on the screen are the same for each location on the source (see § 2.2.3), the average visibility is the ensemble average of Eq. 11, which contains as a factor the Fourier transform of the intensity distribution of the source:

$$\bar{V}(\mathbf{b}) = \frac{1}{\langle I \rangle} \left\langle \sum_{i} \frac{e^{i\phi_{i}}}{H_{i}} e^{-i(k/D)\mathbf{b} \cdot \mathbf{x}_{i}} \sum_{j} \frac{e^{-i\phi_{j}}}{H_{j}} \int_{\text{source}} d\mathbf{s} \, I(\mathbf{s}) \, e^{i(k/R)(\mathbf{x}_{i} - \mathbf{x}_{j}) \cdot \mathbf{s}} \right\rangle$$
(21)

Again, terms with $i \neq j$ have large phases uniformly distributed between 0 and 2π , because the points of stationary phase have uncorrelated phases, and do not survive the ensemble averaging. For terms with i = j, the integral over the source collapses to a factor of the integrated intensity of the source, and the point of stationary phase contributes $1/H_i^2$ to the ensemble average. Thus, the average visibility is the same for a small extended source as it is for a point source, at the same location, and is given by Eq. 20.

If the source is large enough to be resolved by the interferometer in the absence of scattering, it will be large enough that points of stationary phase shift significantly, for different points on the source. In this case each point on the source will have its collection of points of stationary phase, each drawn from a distribution of the form of Eq. 18, each centered on the point where the line of sight to the source intersects the screen. We can take this into account by forming the ensemble average in Eq. 21 before integrating over the source. In the ensemble average, the product of sums will again collapse to products of terms with i = j, producing a scattering disk of the form of Eq. 20 for each point on the

source. The integral over source structure then produces a convolution of this point-source response with the source structure. We thus obtain the well-know fact that the visibility of an extended, spatially incoherent, scattered source is the Fourier transform of the structure of the source, times the visibility of a scattered point source:

$$\bar{V}(\mathbf{b}) = \frac{1}{\langle I \rangle} \int_{\text{source}} d\mathbf{s} \, I(\mathbf{s}) \, P\left(\mathbf{x} - \left(\frac{D}{D+R}\right) \mathbf{s}\right) \, e^{-i(k/D)\mathbf{b} \cdot \mathbf{x}_i} \tag{22}$$

This result is true under quite general assumptions (see, for example, Rickett 1977). In effect, the source structure averages over scintillation patterns to achieve the ensemble average in any single observation.

5. Distribution Functions

5.1. Distribution of intensity for a point source

For a point source, the electric field is given by Eq. 4 as

$$E = \sum_{i} \frac{e^{i\phi_{i}}}{H_{i}}.$$
 (23)

Here, we take $\mathbf{s}=0$ and $\mathbf{p}=0$ without loss of generality. Because the phases of the different points of stationary phase are uncorrelated and the H_i are all approximately equal, the phasor sum has statistics of a random walk. Therefore, the electric field is drawn from a Gaussian distribution in the complex plane: $P_E(E) = \exp\{-|E|^2/I_0\}/\pi I_0$, where I_0 is the mean intensity. The intensity $I = |E|^2$ is drawn from an exponential distribution: $P_I(I) = P_E(\sqrt{I}) |E| (d|E|/dI) = \exp(-I/I_0)/I_0$, as is well known for strong scattering (Scheuer 1968, Rickett 1970, Goodman 1985). The moments of the distribution of I are $\langle I \rangle = I_0$, $\langle I^2 \rangle = 2I_0^2$, and $\langle I^n \rangle = n! I_0^n$.

5.2. Distribution of intensity of a small incoherent source

Now consider the distribution of intensity for a small, spatially-incoherent source. Eq. 10 gives the intensity for arbitrary source structure. Suppose for definiteness that the source has a Gaussian distribution of brightness, with linear size (standard deviation) σ_{ξ} along one axis and σ_{η} along the other. Then Eq. 10 shows that the intensity is:

$$I = \left(\sum_{i} G_{i}\right) \left(\sum_{j} G_{j}^{*}\right) e^{(k/R)^{2} \left\{\xi_{i} \xi_{j} \sigma_{\xi}^{2} + \eta_{i} \eta_{j} \sigma_{\eta}^{2}\right\}}$$

$$(24)$$

where again

$$G_{i} = \frac{e^{i\phi_{i}}}{H_{i}} \exp^{-\frac{1}{2}(k/R)^{2} \{\xi_{i}^{2} \sigma_{\xi}^{2} + \eta_{i}^{2} \sigma_{\eta}^{2}\}}, \tag{25}$$

and where $\mathbf{x}_i = (\xi_i, \eta_i)$. Because of the products in the final factor of Eq. 24, this expression cannot be treated as the square modulus of a random walk.

For sources smaller than the resolution of the scattering disk, acting as a lens, $(k/R)x_i\sigma \ll 1$. In this case we can expand the final factor in Eq. 24 though first order to yield 3 terms:

$$e^{\left((k/R)^2(\xi_i\xi_j\sigma_\xi^2+\eta_i\eta_j\sigma_\eta^2)\right)} \approx 1 + (k/R)(\xi_i\sigma_\xi)(k/R)(\xi_j\sigma_\xi) + (k/R)(\eta_i\sigma_\eta)(k/R)(\eta_j\sigma_\eta). \tag{26}$$

Each of the terms is a product of identical factors depending on \mathbf{x}_i or \mathbf{x}_j . The intensity is then

$$I \approx E_0 E_0^* + E_{1\xi} E_{1\xi}^* + E_{1\eta} E_{1\eta}^* \tag{27}$$

where

$$E_0 = \sum_{i} G_i$$
 $E_{1\xi} = \sum_{i} G_i (k/R) (\xi_i \sigma_{\xi})$ $E_{1\eta} = \sum_{i} G_i (k/R) (\eta_i \sigma_{\eta})$ (28)

Because \mathbf{x}_i runs through many Fresnel zones in strong scattering, and ϕ_i varies greatly within each Fresnel zone, \mathbf{x}_i and ϕ_i are uncorrelated. Therefore the electric fields E_0 , $E_{1\xi}$, and $E_{1\eta}$ have statistics of independent random walks. They are uncorrelated phasors drawn from 3 independent Gaussian distributions. Their square moduli are drawn from

uncorrelated exponential distributions. The net intensity I is thus the sum of 3 independent "intensities," each drawn from a different exponential distribution.

The probability distribution function for I is the convolution of these 3 corresponding exponential distributions, which have exponential scales

$$I_0 = E_0 E_0^* \qquad I_{1\xi} = I_0 (kM\theta\sigma_{\xi})^2 \qquad I_{1\eta} = I_0 (kM\theta\sigma_{\eta})^2$$
 (29)

Here M=D/R plays the role of magnification for a lens. Calculation shows that this convolution is the weighted sum of the 3 exponentials:

$$P(I) = \frac{I_0}{(I_0 - I_{1\xi})(I_0 - I_{1\eta})} \exp\left\{-I/I_0\right\} + \frac{I_{1\xi}}{(I_{1\xi} - I_0)(I_{1\xi} - I_{1\eta})} \exp\left\{-I/I_{1\xi}\right\} + \frac{I_{1\eta}}{(I_{1\eta} - I_{1\xi})(I_{1\eta} - I_0)} \exp\left\{-I/I_{1\eta}\right\}$$
(30)

The probability is normalized to 1: $\int dIP(I) = 1$. For a small source, scales of the second and third exponentials are small, and the distribution function differs from that for a point source only at small intensities. Eq. 30 shows that P(I) = 0 and dP(I)/dI = 0 at I = 0; these facts and normalization yield the correct weighting of the 3 exponentials. The mean intensity for Eq. 30 is

$$\langle I \rangle = \frac{I_0^3 + I_{1\xi}^3 + I_{1\eta}^3}{I_0^2 + I_{1\xi}^2 + I_{1\eta}^2}.$$
 (31)

Similar expressions, with higher powers in the numerator, give the higher moments of the intensity. Figure 3 shows an example of such a distribution. Eq. 30 is consistent with the relation between source size and modulation index derived by Salpeter (1967) and Cohen et al. (1967). Eq. 54 below gives the second moment of I for an incoherent Gaussian-distributed source, and recovers their result.

5.3. Interferometric visibility of a point source: short baselines

Equation 8 gives the interferometric visibility for a point source, which differs from intensity by the factor $e^{i(k/D)\mathbf{b}\cdot\mathbf{x}_i}$. When the baseline is short compared with the scale of the

diffraction pattern, so that $kbx/D \ll 1$, then $e^{i(k/D)\mathbf{b}\cdot\mathbf{x}_i} \approx 1 - i(k/D)\mathbf{b}\cdot\mathbf{x}_i$, and

$$C_{AB}(\mathbf{b}) = E_0 E_0^* + E_{1b} E_0^* \tag{32}$$

where E_0 is the electric field observed at the reference station, and

$$E_{1b} = -\sum_{i} \frac{e^{i\phi_{i}}}{H_{i}} i(k/D) \mathbf{b} \cdot \mathbf{x}_{i}. \tag{33}$$

From the preceding sections, we know the distributions of E_0 and $I_0 = E_0 E_0^*$. Note that, like E_0 , E_{1b} is the sum of many phasors, of random lengths and phases. Thus, E_{1b} will be drawn from a Gaussian distribution. Moreover, E_{1b} will be independent of E_0 because the factor $-i(k/D) \mathbf{b} \cdot \mathbf{x}_i$ changes the lengths of the phasors by an amount proportional to \mathbf{x}_i , which is uncorrelated with ϕ_i .

The probability density function for E_1 is

$$P(E_1) = \frac{1}{2\pi\delta^2} \exp\{-\frac{1}{2}(|E_1|^2/I_0^2\delta^2)\}$$
 (34)

where

$$\delta^2 = \left\langle ((k/D)\,\mathbf{b}\cdot\mathbf{x}_i)^2 \right\rangle_i = (k\theta b)^2 \tag{35}$$

Here, as in Eq. 18, $\langle ... \rangle_i$ indicate an average over an ensemble of screens, with points weighted by $1/H_i^2$.

We calculate the distribution function for C_{AB} by convolving the exponential distribution function for $I = E_0 E_0^*$ with the Gaussian distribution for E_{1b} , scaled by E_0 . The result is

$$P(C_{AB}) = \frac{1}{2\pi} \frac{2}{I_0 \delta^2} \exp\left(\frac{\text{Re}(C_{AB})}{I_0 \delta^2}\right) K_0 \left(\sqrt{\frac{2}{\delta^2} + \frac{1}{\delta^4}} \frac{|C_{AB}|}{I_0}\right).$$
(36)

Here K_0 is the modified Bessel function of the second kind, of order 0. Figure 4 shows a sample plot of the distribution function $P(C_{AB})$. To a reasonable approximation, $P(C_{AB})$ is nearly an exponential along the real axis, convolved with a Gaussian along the imaginary

direction. The exponential scale of the real part is the mean intensity, I_0 . The variance of the imaginary part, at a given value of the real part of C_{AB} , is proportional to the square of the real part, and to $(k/R)\theta b$, the baseline length in units of the scale of the diffraction pattern. Thus, the imaginary part varies most when the real part is large; but the largest phase variations are found when the real and imaginary parts are small.

6. Fourth Moments

Fourth moments of the electric field provide readily observable quantities. These quantities include the decorrelation bandwidth of scintillation and the modulation index. In this section, we derive moments appropriate for arbitrary source structure and scattering screens, and simpler forms appropriate for Gaussian source structures.

6.1. Decorrelation bandwidth for a point source

The scintillation pattern changes with observing frequency. This change is usually characterized by the decorrelation bandwidth $\Delta\nu_d$, the half-width at half-maximum of the correlation function of intensity I, expressed as a frequency difference ν . In this work, for convenience we use wavenumber $k = 2\pi\nu/c$ and decorrelation wavenumber $\Delta k_H = 2\pi\Delta\nu_d/c$.

We define the delay for the ith point of stationary phase, τ_i , by $c\tau_i = x_i^2 \left[\frac{1}{2R} + \frac{1}{2D}\right] + \frac{1}{k}\Phi(\mathbf{x}_i)$. This delay is the extra time for a signal to propagate via that point, rather than directly through the center of the screen. To a good approximation, in strong scattering, and particularly for interstellar radio-wave scattering, we can ignore the screen contribution to τ_i in favor of the much larger geometric delay. In terms of τ_i , the electric field of a point

source is

$$E(k) = \sum_{i} \frac{1}{H_i} e^{-ikc\tau_i},\tag{37}$$

and the intensity is

$$I(k) = \sum_{ij} \frac{1}{H_i} e^{-ikc\tau_i} \frac{1}{H_j} e^{ikc\tau_j}, \tag{38}$$

where we set $\mathbf{p} = 0$ without loss of generality.

We consider autocorrelation functions of intensity with wavenumber difference Δk :

$$\left\langle I(k)I(k+\Delta k)\right\rangle = \left\langle \sum_{ij\ell m} \frac{1}{H_i} e^{-ikc\tau_i} \frac{1}{H_j} e^{ikc\tau_j} \frac{1}{H_\ell} e^{-ikc\tau_\ell} \frac{1}{H_m} e^{ikc\tau_m} e^{-i\Delta kc\tau_\ell} e^{i\Delta kc\tau_m} \right\rangle. \tag{39}$$

Because the phases ϕ_i are uncorrelated, as discussed in § 2.2, only terms with either i = j and $\ell = m$, or with i = m and $j = \ell$, will survive the ensemble average, so that

$$\left\langle I(k)I(k+\Delta k)\right\rangle = \left\langle I\right\rangle^2 + \left\langle \sum_{ij} \frac{1}{H_i^2} \frac{1}{H_j^2} e^{i\Delta k c(\tau_i - \tau_j)} \right\rangle \tag{40}$$

The case i = j gives the first term, which is independent of Δk ; the case i = m gives the second term. We find the expected value of the average by integrating over the probability density function $P(\mathbf{x})$ given by Eq. 18, parallel to the approach of § 4. Note that $P(\tau) = P(\mathbf{x})(d\tau/d\mathbf{x})^{-1}$. Because $P(\mathbf{x})$ follows a Gaussian distribution, $P(\tau)$ follows an exponential distribution: $P(\tau) = \frac{1}{\tau_0}e^{-\tau/\tau_0}$, where $c\tau_0 = \left[\frac{1}{D} + \frac{1}{R}\right]\theta^2 D^2$. We thus find that the autocorrelation function follows a Lorentzian distribution, plus 1:

$$\frac{1}{\langle I \rangle^2} \langle I(k)I(k+\Delta k)\rangle = 1 + \frac{1}{1 + (\Delta k c \tau_0)^2}.$$
 (41)

The half width at half maximum of the Lorentzian is

$$\Delta k_H = \frac{2\pi\Delta\nu_d}{c} = \frac{1}{c\tau_0} = \left[\frac{1}{D} + \frac{1}{R}\right]^{-1} \frac{1}{D^2} \frac{1}{\theta^2}.$$
 (42)

Note that, approximately, $\Delta k_H/k \approx r_d^2/r_F^2$. This is in agreement with calculations based on other approaches (Rickett 1977, Gupta 1995). The fact that the electric field in Eq. 37 is a Gaussian random variable with zero mean can simplify this calculation; however, when the source is extended, the E does not follow a Gaussian distribution, as §5.2 makes clear.

6.2. Decorrelation bandwidth for an incoherent source

If the source has finite size and is incoherent, the Fourier transform of its intensity distribution will appear in the expression for the intensity of the scintillation pattern, as Eq. 10 shows. The product of two Fourier transforms will thus appear in the autocorrelation of the intensity:

$$\langle I(k)I(k+\Delta k)\rangle = \langle I\rangle^{2} + \left\langle \sum_{i,j} \frac{1}{H_{i}^{2}} \frac{1}{H_{j}^{2}} e^{i\Delta ck(\tau_{j}-\tau_{i})} \int d\mathbf{s}_{1} e^{i(k/R)(\mathbf{x}_{j}-\mathbf{x}_{i})\cdot\mathbf{s}_{1}} I(\mathbf{s}_{1}) \right.$$

$$\times \int d\mathbf{s}_{2} e^{-i((k+\Delta k)/R)(\mathbf{x}_{j}-\mathbf{x}_{i})\cdot\mathbf{s}_{2}} I(\mathbf{s}_{2}) \left. \right\rangle. \tag{43}$$

In strong scattering, the bandwidth of the scintillation pattern is much less than the observing frequency.

If the angular size of the source is smaller than the angular size of the scattering disk, then $(\Delta k/R)\theta D$ s << 1, for points s on the source. Thus,

$$\langle I(k)I(k+\Delta k)\rangle = \langle I\rangle^2 + \left\langle \sum_{i,j} \frac{1}{H_i^2} \frac{1}{H_j^2} e^{i\Delta k c(\tau_j - \tau_i)} \left| \int d\mathbf{s} \, e^{i(k/R)(\mathbf{x}_j - \mathbf{x}_i) \cdot \mathbf{s}} I(\mathbf{s}) \right|^2 \right\rangle. \tag{44}$$

Again the Fourier transform of source structure appears. A typical pair of points of stationary phase on the screen, with separation about θD , will sample source structure with spatial frequency $k(D/R)\theta$. For a source of limited size, relative to the corresponding length $\lambda(R/D)/\theta$, I(s) will decline for large s. Thus, points of stationary phase with large separation will contribute less to the sum than they would for a point source. For a point source, these pairs of points with large separations limit the bandwidth of the scintillation pattern, because they produce large differences in travel time τ . When finite source size makes such points contribute less, we expect the decorrelation bandwidth to broaden.

As a simple example, suppose that the source has a circular Gaussian distribution of intensity. By substituting Eq. 12 into Eq. 44 and evaluating the integrals, with the assumption that the distribution of points of stationary phase follows a Gaussian

distribution, we obtain an expression of the form of Eq. 41:

$$\frac{1}{\langle I \rangle^2} \langle I(k)I(k+\Delta k) \rangle = 1 + \frac{1}{1 + 4\sigma_1^2 + (\Delta k c \tau_0)^2},\tag{45}$$

where the size of the source, in units of the linear resolution of a lens with diameter of the scattering disk, is $\sigma_1 = k(D/R)\theta\sigma$. This is equivalent to the expression derived by Chashei & Shishov (1976). The autocorrelation function of intensity $\langle I(k)I(k+\Delta k)\rangle$ again follows a Lorentzian distribution, but now with half-width at half-maximum

$$\Delta k_H = (2\pi/c)\Delta\nu_d = (1/c\tau_0)\sqrt{1+4\sigma_1^2}$$
(46)

The finite size of the source increases the decorrelation bandwidth, as expected.

6.3. Decorrelation bandwidth for interferometric visibility

The interferometric visibility C_{AB} is complex. Several correlation functions can be formed from it. Among these are $\langle C_{AB}C_{AB}^* \rangle$ and $\langle C_{AB}C_{AB} \rangle$. Both of these function are real. From these we can calculate correlation functions for the real and imaginary parts, and their cross-correlation.

For the correlation function $\langle C_{AB}(k)C_{AB}^*(k+\Delta k)\rangle$, the effects of nonzero baseline are completely decoupled from those of frequency difference and of source structure. For this function, we find:

$$\frac{1}{\langle I \rangle^2} \langle C_{AB}(k) C_{AB}^*(k + \Delta k) \rangle = \bar{V}(\mathbf{b})^2 - 1 + \frac{1}{\langle I \rangle^2} \langle I(k) I(k + \Delta k) \rangle, \tag{47}$$

where Eq. 17 gives the normalized average visibility for a point source, $\bar{V}(\mathbf{b})$, and Eq. 41 or 45 gives the autocorrelation function of intensity $\langle I(k)I(k+\Delta k)\rangle$. Thus, for this correlation function, decorrelation bandwidth is independent of baseline length. Note that this fact is true for arbitrary source structure.

As a specific example, consider a source with Gaussian intensity distribution, with standard deviations σ_{ξ} and σ_{η} along the directions ξ and η . For such a source,

$$\frac{1}{\langle I \rangle^2} \langle C_{AB}(k) C_{AB}^*(k + \Delta k) \rangle = \exp\left\{ -(k\theta b)^2 \right\} + f_{\xi} f_{\eta}, \tag{48}$$

where the function f_{ξ} is defined by:

$$f_{\xi} = \left\{ 1 + 4\sigma_{1\xi}^2 + (\Delta k c \tau_0)^2 \right\}^{-1/2} \tag{49}$$

and where we have used the definitions:

$$\tau_0 = \frac{1}{c} \left[\frac{1}{D} + \frac{1}{R} \right] D^2 \theta^2$$

$$\sigma_{1\xi} = k(D/R)\theta \sigma_{\xi}$$
(50)

The same expressions, with η substituted for ξ , define the function f_{η} .

The correlation function $\langle C_{AB}(k)C_{AB}(k+\Delta k)\rangle$ mixes dependences on baseline, frequency, and source structure. For an source of finite size, observed on nonzero baseline,

$$\frac{1}{\langle I \rangle^{2}} \left\langle C_{AB}(k) C_{AB}(k + \Delta k) \right\rangle = \bar{V}(\mathbf{b})^{2} + \left\langle \sum_{i,j} \frac{1}{H_{i}^{2}} \frac{1}{H_{j}^{2}} e^{i(k/R)\mathbf{b} \cdot (\mathbf{x}_{j} - \mathbf{x}_{i})} \right. \tag{51}$$

$$e^{i\Delta kc(\tau_{j} - \tau_{i})} \left| \int d\mathbf{s} \ e^{i(k/D)(\mathbf{x}_{j} - \mathbf{x}_{i}) \cdot \mathbf{s}} I(\mathbf{s}) \right|^{2} \right\rangle.$$

The seond term depends on baseline **b** as well as wavenumber difference Δk , so that for this correlation function, decorrelation bandwidth does depend on baseline length.

For an elliptical-Gaussian source, the correlation function takes the form

$$\frac{1}{\langle I \rangle^2} \langle C_{AB}(k) C_{AB}(k + \Delta k) \rangle = \exp\left\{ -(k\theta b)^2 \right\} + g_{\xi} g_{\eta}$$
 (52)

where the function g_{ξ} is defined by:

$$g_{\xi} = \left\{ 1 + 4\sigma_{1\xi}^2 + \Delta k^2 c^2 \tau_0^2 \right\}^{-1/2} \exp\left\{ \frac{-(1 + 4\sigma_{1\xi}^2)(k\theta b_{\xi})^2}{1 + 4\sigma_{1\xi}^2 + \Delta k^2 c^2 \tau_0^2} \right\}$$
 (53)

and we use the definitions for τ_0 and $\sigma_{1\xi}$ from Eq. 50 above. The same expressions, with η substituted for ξ , define the function g_{η} . Figure 5 shows examples of the distributions of $\langle C_{AB}(k)C_{AB}^*(k+\Delta k)\rangle$ and $\langle C_{AB}(k)C_{AB}(k+\Delta k)\rangle$ as functions of baseline b and decorrelation wavenumber Δk , for a point source.

The correlation functions for interferometric visibility yield several interesting limits. For a baseline of zero length (b=0) but with no difference in frequency $(\Delta k=0)$, we recover from Eq. 48 or 52 the expression for the modulation index of a Gaussian source (Salpeter 1967, Cohen et al. 1967, Gwinn et al. 1997):

$$\frac{1}{\langle I \rangle^2} \langle I^2 \rangle - 1 = m^2 = \left(1 + 4\sigma_{1\xi}^2 \right)^{-1/2} \left(1 + 4\sigma_{1\eta}^2 \right)^{-1/2}. \tag{54}$$

For baseline of zero length (b = 0) but with nonzero frequency difference $(\Delta k \neq 0)$, we recover the correlation function for a Gaussian source, Eq. 45, but now including effects of departures from circularity. With arbitrary baseline, but with zero source size and zero frequency difference, we obtain the second moments of the visibility for a point source:

$$\frac{1}{\langle I \rangle^2} \langle C_{AB} C_{AB} \rangle = 2 \exp \left\{ - (k\theta b)^2 \right\}
\frac{1}{\langle I \rangle^2} \langle C_{AB} C_{AB}^* \rangle = \exp \left\{ - (k\theta b)^2 \right\} + 1.$$
(55)

From these we can calculate the second moments of the real and imaginary parts:

$$\frac{1}{\langle I \rangle^2} \langle \operatorname{Re} \left[C_{AB} \right]^2 \rangle = \frac{1}{2} + \frac{3}{2} \exp \left\{ -(k\theta b)^2 \right\}
\frac{1}{\langle I \rangle^2} \langle \operatorname{Im} \left[C_{AB} \right]^2 \rangle = \frac{1}{2} - \frac{1}{2} \exp \left\{ -(k\theta b)^2 \right\}$$
(56)

These expressions are the moments of the probability distribution function given in Eq. 36, but here we do not assume that that $k\theta b \ll 1$. These moments can be used to find the angular broadening θ from observations of C_{AB} in the speckle limit. Equivalently, we can determine the phase structure function $D_{\phi}(\mathbf{b}) \approx (k\theta b)^2$ Using Eq. 20 for $\langle C_{AB} \rangle = \langle \text{Re} [C_{AB}] \rangle$,

we find approximate expressions for $D_{\phi}(\mathbf{b})$ for short baselines:

$$D_{\phi}(\mathbf{b}) \approx 2 \frac{\langle \operatorname{Im} \left[C_{AB} \right]^{2} \rangle}{\langle \operatorname{Re} \left[C_{AB} \right] \rangle} \approx 4 \frac{\langle \operatorname{Im} \left[C_{AB} \right]^{2} \rangle}{\langle \operatorname{Re} \left[C_{AB} \right]^{2} \rangle}$$
 (57)

Thus, measurements of the real and imaginary parts of C_{AB} , on short baselines, yield θ . This technique has been used to measure angular broadening of pulsars, and so infer the location of scattering material along the line of sight (Desai et al. 1992, Britton 1997, Britton, Gwinn, & Ojeda 1998). The approximation is good as long as the baseline is short, relative to the scale of the diffraction pattern in the plane of the observer.

7. Scattering of Beams from Spatially-Coherent Sources

In this section we consider scattering of a beam of radiation that does not illuminate the entire scattering disk. In practice, a variety of configurations at the source can result in non-uniform illumination at the scattering disk. In the context of our formalism, where the source lies on a thin screen, variations in intensity over the scattering disk arise from spatial coherence at the source. In this narrow sense, masers, pulsars, and relativistically-expanding sources are spatially coherent, because their radiation patterns are non-uniform. A spatially coherent source will, in general, produce a non-uniform intensity pattern in the observer plane. This is a consequence of the generalized Van Cittert-Zernicke theorem (Born & Wolf 1980, Goodman 1985).

Non-uniform intensity is important for interstellar scattering only if the source illuminates the scattering disk unevenly. As a simple model of this situation, we explore scattering of a source that produces a beam of radiation with a Gaussian profile. We then discuss the generalization of this model to more complicated partially spatially coherent sources.

7.1. Beam from a Fully Coherent Source

For a completely coherent source, the electric field is identical at different points, possibly with varying amplitude and phase. As a simple model of a spatially-coherent source, we consider a source with electric field

$$E(\mathbf{s}) = E(0) e^{-\frac{1}{4}(s/\sigma_C)^2} e^{-i(k/R)\mathbf{x}_0 \cdot \mathbf{s}}$$
(58)

This source has a Gaussian intensity profile, with standard deviation σ_C , and is perfectly coherent. Here E(0) is an arbitrary complex constant that depends on observing frequency, and \mathbf{x}_0 is a frequency-independent vector. Eq. 2 shows that this source will produce a Gaussian beam, centered at \mathbf{x}_0 on the scattering screen, with standard deviation $(k\sigma_C/R)^{-1}$. The beam will illuminate the scattering disk if $\mathbf{x}_0 \lesssim \theta D$, and the illumination will be non-uniform if $\sigma_C > R/k\theta D$; in other words, if the linear resolution of the scattering disk, viewed as a lens, is finer than the scale of spatial coherence of the source.

The interferometric visibility will be:

$$C_{AB} = \left(\sum_{i} \frac{e^{i\phi_{i}}}{H_{i}} e^{-(k\sigma_{C}/R)^{2} x_{0i}^{2}} e^{-i(k/D)\mathbf{b}\cdot\mathbf{x}_{0i}}\right) \left(\sum_{j} \frac{e^{-i\phi_{j}}}{H_{j}} e^{-(k\sigma_{C}/R)^{2} x_{0j}^{2}}\right) e^{-i(k/D)\mathbf{b}\cdot\mathbf{x}_{0}}, \quad (59)$$

where $\mathbf{x}_{0i} = \mathbf{x}_i - \mathbf{x}_0$ is the offset of the point of stationary phase from the center of the beam. As this expression shows, the beam illuminates only part of the scattering disk, leading to smaller angular broadening and a phase offset. Comparison with Eq. 13 shows that a Gaussian beam differs from an incoherent source of the same size in that the sums remain uncorrelated, and that the scattering disk is more strongly vignetted, by a factor of 2.

7.2. Beam from a partially spatially coherent source

Most coherent sources exhibit only partial spatial coherence. Moreover, Ishimaru (1978, §20-7) points out that an initially collimated, spatially-coherent beam traveling through a scattering medium will lose its spatial coherence more rapidly than it will lose its collimation. To characterize mutual coherence, we introduce the cross-spectral density function (Goodman 1985):

$$\mathcal{G}_{12}(k) = \langle E(\mathbf{s}_1, k) E^*(\mathbf{s}_2, k) \rangle_{1/B}. \tag{60}$$

Again the subscripted angular brackets $\langle ... \rangle_{1/B}$ indicate averaging in time t over many inverse observing bandwidths. As a simple model for a source with partial spatial coherence, we consider a source with Gaussian intensity distribution with standard deviation σ , and with cross-spectral density function

$$\mathcal{G}_{12}(k) = \frac{I_0}{8\pi\mu^2} \exp\left\{-\frac{(\mathbf{s}_1 - \mathbf{s}_2)^2}{8\mu^2}\right\} e^{\{-i(k/R)\mathbf{x}_0\cdot(\mathbf{s}_1 - \mathbf{s}_2)\}} e^{-\frac{1}{4}(s_1/\sigma)^2} e^{-\frac{1}{4}(s_2/\sigma)^2}$$
(61)

Such a source has partial spatial coherence and produces a Gaussian beam. The scale of coherence at the source is μ . This expression becomes that for a fully spatially-incoherent Gaussian source of size σ , Eq. 9, for $\mu \to 0$, and becomes that for a fully-coherent source that emits a Gaussian beam (Eq. 58 above with $\sigma_C = \sigma$), for $\mu \to \infty$. The expression is easily generalized to the case of anisotropic cross-spectral density function with scales of spatial coherence μ_{ξ} and μ_{η} along the 2 axes; or to more complicated expressions when these axes are not aligned with the coordinate directions ξ and η .

We can use the cross-spectral density function in the same way as the assumption of complete spatial incoherence, Eq. 9 above, to find the electric field at the observer. The expression for the interferometric visibility becomes:

$$C_{AB} = \left(\sum_{i} G_{0i} e^{-i(k/R)\mathbf{b}\cdot(\mathbf{x}_{0i})}\right) \left(\sum_{j} G_{0j}^{*}\right) e^{(k/R)^{2}\sigma_{P}^{2}\mathbf{x}_{0j}\cdot\mathbf{x}_{i}} e^{-i(k/R)\mathbf{b}\cdot\mathbf{x}_{0}}, \tag{62}$$

where $\mathbf{x}_{0i} = \mathbf{x}_i - \mathbf{x}_0$ is the location of the stationary-phase point with respect to the center of the beam from the source, and the reweighted phasor is

$$G_{0i} = \frac{e^{i\phi_i}}{H_i} e^{-\frac{1}{2}(k/R)^2 \sigma_W^2 x_i^2}.$$
(63)

In these expressions, $\sigma_P^2 = \sigma^4/(\sigma^2 + \mu^2)$ plays the role of σ in the correlations between sums over i and j, and $\sigma_W^2 = (\sigma^4 + 2\sigma^2\mu^2)/(\sigma^2 + \mu^2)$ plays that role in reweighting the phasors. Compared with θ for a spatially-incoherent source of the same size (Eqs. 13 and 14), the effective size of the scattering disk for our partially-coherent source is θ_W , where

$$\frac{1}{\theta_W^2} = \frac{1}{\theta^2} + 2(kD/R)^2 \sigma^2 \left(\frac{\sigma^2 \mu^2}{\sigma^2 + \mu^2}\right).$$
 (64)

Except for the facts that $\sigma_P \neq \sigma$, $\theta_W \neq \theta$, and the overall phase factor $e^{-i(k/R)\mathbf{b}\cdot\mathbf{x}_0}$, Eq. 62 is identical to Eq. 13; in the limit $\mu \to 0$ they become identical. The intensity is the same expression, with $\mathbf{b} = 0$.

7.3. Effects of Nonuniform Illumination

The preceding section shows that beamed radiation offsets the scattering disk, introducing a phase offset, and reduces its aperture, as compared to a point source. Beaming also reduces the effective size of an extended source, and reduces the size of the scattering disk. A smaller scattering disk corresponds to higher visibility on long baselines, smaller phase variations, and a broader decorrelation bandwidth. A smaller source size corresponds to narrower decorrelation bandwidth and modulation index closer to 1. For these effects to be important for interstellar scattering, the source must possess spatial coherence on a scale sufficient to resolve the scattering disk: the mutual coherence function $\mathcal{G}_{12}(k)$ must be nonzero for separations $|\mathbf{s}_1 - \mathbf{s}_2| \approx \lambda/(D/R)\theta$. These effects change the results of § 3 thorugh 6, which were derived for purely incoherent, unbeamed sources, by changing θ to θ_W and σ to σ_P , and by changing the average phase of the visibility. While

these results are true for a specific, simple model, we may expect that, in general, sources that illuminate the scattering disk non-uniformly will produce similar effects.

We expect that the beam will not remain directed at the same point on the scattering disk for long: changes in the structure of the source, or rotation in the case of pulsars, will carry the beam across the scattering disk. In this case we expect observations to sample the sum of many beams, each directed at some point on the screen. In the limit of observations over many independent pulses, for example, we expect that a large number of beams will illuminate the entire scattering disk, restoring the observables expected for an unbeamed source.

8. Summary

We present the Kirchoff integral for the diffraction pattern of a source scattered by a thin screen, and use the stationary phase approximation to express the integral as a phasor sum, multiplied by an integral over the source, in strong scattering. For a point source, intensity is the square of a phasor sum, and interferometric visibility is the product of two different phasor sums. Finite source size introduces correlations between terms in the two sums.

Using this formalism we explore the effects of source structure on the scattered radiation. We calculate the distribution of intensity for a small source, and find that it is the sum of 3 exponentials, with the largest difference from that for a point source at the lowest intensities. Similarly, we calculate the distribution of interferometric visibility of a point source observed on a baseline shorter than the characteristic scale of the diffraction pattern. This distribution is approximately an exponential, for the real part, and a Gaussian distribution for the imaginary part.

We present expressions for the correlation of intensity with wavenumber $\langle I(k)I(k+\Delta k)\rangle/\langle I\rangle$. We find Lorentzian distributions for a point source or an extended Gaussian source. We find that extended sources have greater decorrelation bandwidth than point sources, for the same scattering screen.

We also calculate the correlation function for interferometric visibility with wavenumber. Because interferometric visibility C_{AB} is complex, the correlation functions $\langle C_{AB}(k)C_{AB}(k+\Delta k)\rangle$ and $\langle C_{AB}(k)C_{AB}^*(k+\Delta k)\rangle$ are different. Both show an overall decrease in correlation with increasing baseline length and with increasing frequency difference Δk . The correlation function $\langle C_{AB}(k)C_{AB}^*(k+\Delta k)\rangle$ contains no information on source structure beyond that carried by the correlation function for intensity, $\langle I(k)I(k+\Delta k)\rangle/\langle I\rangle$. The decorrelation bandwidth is independent of baseline length, for this function.

The function $\langle C_{AB}(k)C_{AB}(k+\Delta k)\rangle$ carries information about source structure. It involves the projection of the source, along the direction of the baseline, and so offers the possibility of sampling the 2-dimensional structure of the source on the sky. We derive various simple limits of the correlation functions for interferometric visibility. From these limits we can obtain information on the size of the source and the angular size of the scattering disk.

We discuss scattering of beams of radiation, from sources that are, in our formalism, spatially coherent. We find that these beams "vignette" the scattering disk, and so effectively have smaller angular broadening than a point source, or a spatially-coherent source of the same size, scattered by the same screen. A beam from an extended, partially coherent source has effects equivalent to those of a smaller incoherent source, seen through a smaller scattering disk.

We thank W.L. Coles, B.J. Rickett, and M.A. Walker for stimulating conversations. We thank the U.S. National Science Foundation for support.

REFERENCES

Armstrong, J.W., & Coles, W.L. 1978, ApJ, 220, 346

Backer, D.C. 1975, A&A, 43, 395

Beckers, J.M., 1993, ARA&A, 31, 13

Born, M., & Wolf, E. 1980, Principles of Optics (Oxford: Pergamon)

Britton, M.C. 1997, PhD Thesis, University of California, Santa Barbara

Britton, M.C., Gwinn, C.R., & Ojeda, M.J. 1997, ApJ, in press

Chashei, I.V., & Shishov, V.I. 1976, Sov Ast, 20, 13

Cohen, M.H., & Cronyn, W.M. 1974, ApJ, 192 193

Cohen, M.H., Gundermann, E.J., & Harris, D.E. 1967, ApJ, 150, 767

Codona, J.L., Creamer, D.B., Flatté, S.M., Frehlich, R.G., & Henyey, F.S. 1986, Radio Science, 21, 805

Cordes, J.M., Weisberg, J.M., & Boriakoff, V. 1983, ApJ, 268, 370

Cordes, J.M., Weisberg, J.M., & Boriakoff, V. 1985, ApJ, 288, 221

Cornwell, T.J., Anantharamaiah, K.R., & Narayan, R. 1989, JOSA, A 6, 977

Cornwell, T.J., & Napier, P.J. 1988, Radio Sci, 23, 739-748

Cornwell, T.J., & Narayan, R. 1993, ApJ, 408, L69

Desai, K.M., Gwinn, C.R., Reynolds, J.R., King, E.A., Jauncey, D., Flanagan, C., Nicolson, G., Preston, R.A., & Jones, D.L. 1992, ApJ, 393, L75

Desai, K.M., Gwinn, C.R., & Diamond, P.J. 1995, Nature, 372, 754

Goldreich, P., Sridhar, S. 1995, ApJ, 438, 763

Goodman, J.W. 1985, Statistical Optics, New York: Wiley

Goodman, J.W. 1968, Introduction to Fourier Optics, New York: McGraw-Hill

Gupta, Y. 1995, ApJ, 451, 717

Gwinn, C.R., Cordes, J.M., Bartel, N., Wolszczan, A., & Mutel, R.L. 1988, ApJ, 334, L13

Gwinn, C.R., Moran, J.M., & Reid, M.J. 1990, Radio Astronomical Seeing, ed. J. Baldwin & Wang Shoguan, International Academic Publishers, Beijing.

Gwinn, C.R., Ojeda, M.J., Britton, M.C., Reynolds, J.R., Jauncey, D.L., King, E.A., McCulloch, P.M., Lovell, J.E.J., Flanagan, C.S., Smits, D.P., Preston, R.A., & Jones, D.L. 1997, ApJ, 485, L87

Hajivassiliou, C.A. 1992, Nature, 355, 232

Hewish, A., Readhead, A.C.S., & Duffett-Smith, P.J., 1974, Nature, 252, 657

Higdon, J.C. 1984, ApJ, 285, 109

Ishimaru, A. 1978, Wave Propagation and Scattering in Random Media, v. 2, New York:

Academic Press

Jackson, J.D. 1975, Classical Electrodynamics, 2nd ed., New York: Wiley

Lee, L.C., & Jokipii, J.R., 1976, ApJ, 206, 735

Montgomery, D., Brown, M.R., and Matthaeus, W.H., 1987, JGR, 92, 282

Molnar L.A., Mutel R.L., Reid M.J., Johnston, K.J. 1995, ApJ, 438, 708

Moran, J.M., Rodríguez, L.F., Greene, B., & Backer, D.C. 1990, ApJ, 348 147

Narayan, R. & Goodman, J. 1989, MNRAS, 238, 963

Pearson, T.J., & Readhead, A.C.S. 1984, ARA&A, 21, 97

Rao, A.P., & Ananthakrishnan, S. 1984, Nature 312 707

Readhead, A.C.S., & Duffett-Smith, P.J., 1977, A&A, 42, 151

Rickett, B.J. 1970, MNRAS, 150, 67

Rickett, B.J., 1977, ARA&A, 15, 479

Roggemann, M. C., Welsh, B. M., & Fugate, R. Q. 1997, Rev Mod Phys, 69, 2, 437

Rumsey, V.H. 1975, Radio Science, 10, 107

Salpeter, E.E. 1967, ApJ, 147, 433

Scheuer, P.A.G. 1968, Nature, 218, 920

Smirnova, T. V., Shishov, V. I., Malofeev, V. M. 1996, ApJ, 462, 289

Spangler, S.R., & Gwinn, C.R. 1990, ApJ, 353, L29

Trotter, A.S., Moran, J.M., & Rodriguez, L.F. 1998, ApJ, 493, 666

Wilkinson, P.N., Narayan, R. & Spencer, R.E., 1994, MNRAS, 269, 67

Wolszczan, A. & Cordes, J.M. 1987, ApJ, 320, L35

Wolszczan, A., Bartlett, J.E., & Cordes, J.M. 1988, in Radio Wave Scattering in the Interstellar medium, eds. J.M. Cordes, B.J. Rickett & D.C. Backer (AIP), 145

This manuscript was prepared with the AAS LATEX macros v4.0.

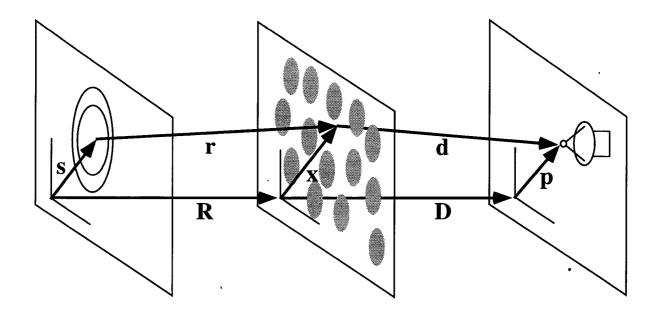


Fig. 1.— Geometry for Kirchoff diffraction by material in a thin screen with a random index of refraction. Radiation from location \mathbf{s} on the source travels along path \mathbf{r} to scattering material at location \mathbf{x} . The radiation suffers a random phase change $\Phi(\mathbf{x})$, and propagates onward to the observer plane along \mathbf{d} , where the observer measures the electric field at location \mathbf{p} . The separation of source plane and screen is \mathbf{R} , and that of screen and observer plane is \mathbf{D} .

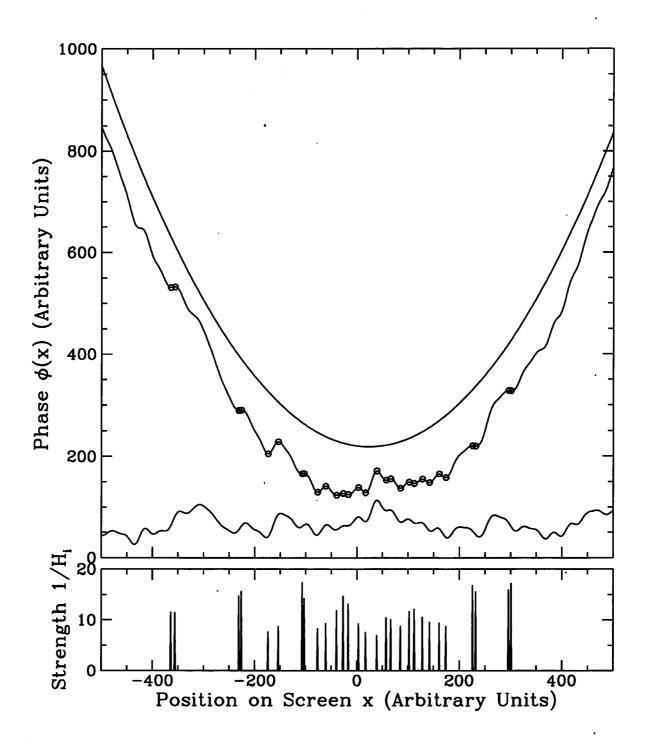


Fig. 2.—

Fig. 2.— Model scattering screen and resulting points of stationary phase for a 1-dimensional screen. Upper: Phase $\phi(x)$ of the transmission function plotted with position on screen x. The upper, parabolic curve shows the geometric phase, $k[\frac{1}{2D} + \frac{1}{2R}]x^2$. The lower, random curve shows the screen phase $\Phi(x)$. The middle, irregular parabolic curve shows the net screen plus geometric phase, $\phi(x)$. Small circles mark points of stationary phase. Lower: Strengths of points of stationary phase on the screen. The increasing slope of the geometric phase far from the center of the screen limits the points of stationary phase to a finite region on the screen: the "scattering disk". In this example, the spectrum of phase variations is a power-law, with index of 5/3, the one-dimensional analog of the 3-dimensional Kolmogorov index of 11/3. The spectrum terminates at a minimum wavelength, or "inner scale", of $\Delta x = 6$. Thus, in this illustration the inner scale is a far larger fraction of scattering disk size than it is in interstellar scattering, and consequently the number of points of stationary phase is far less. Adapted from Britton (1997).

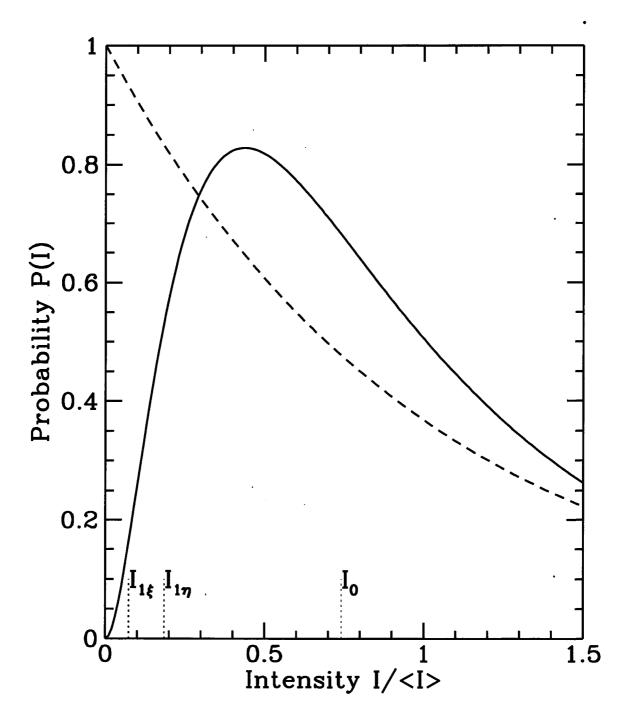


Fig. 3.— Distribution function of intensity of scintillations for a small, extended source (solid line) and for a point source (dashed line). Both distribution functions are normalized to unit area and to mean intensity $\langle I \rangle = 1$. The extended source has a Gaussian distribution of intensity, with variances $\sigma_{\xi}^2 = 0.1 \lambda \theta / 2\pi M$ and $\sigma_{\eta}^2 = 0.25 \lambda \theta / 2\pi M$. The corresponding

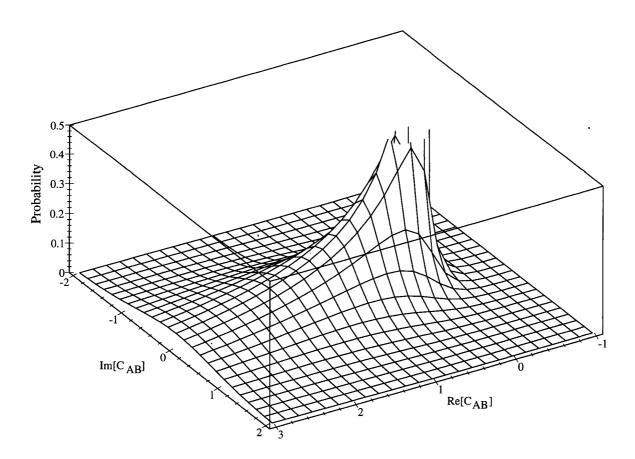


Fig. 4.— Probability distribution function of the interferometric visibility C_{AB} . For this example, $\delta = k\theta b = 0.5$ sets the baseline length at half the scale of the scintillation pattern. Note that the distribution is approximately exponential along the Re $[C_{AB}]$ axis, and is approximately Gaussian for the imaginary part, perpendicular to that axis. The standard deviation of the Gaussian is proportional to the square root of the real part.

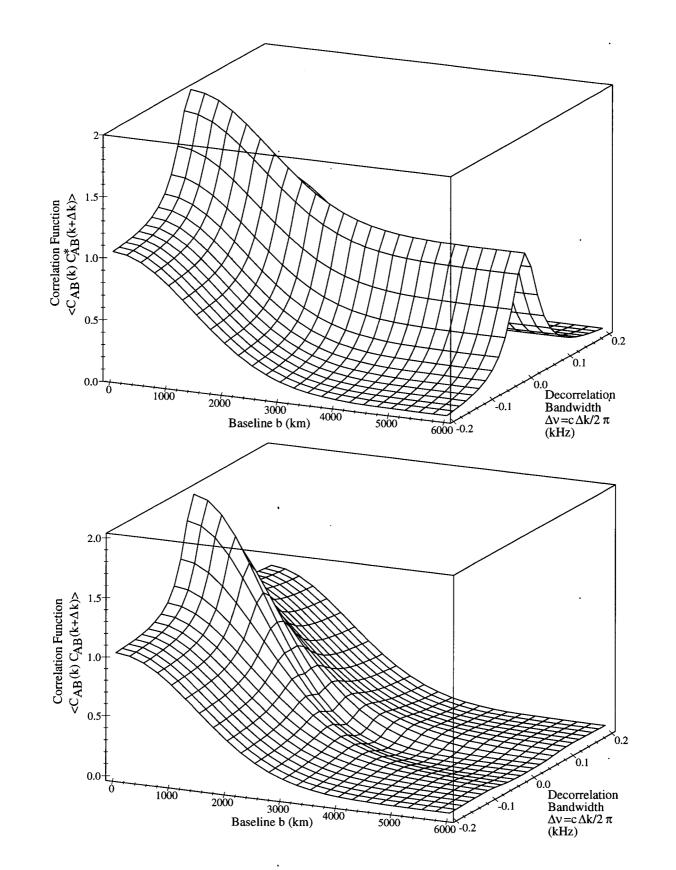


Fig. 5.—

Fig. 5.— Distribution of the correlation functions for interferometric visibility, plotted with baseline length and difference in observing wavenumber Δk (or difference in observing frequency $\Delta \nu$). Upper: Correlation function $\langle C_{AB}(k)C_{AB}^*(k+\Delta k)\rangle$. Lower: Correlation function $\langle C_{AB}(k)C_{AB}(k+\Delta k)\rangle$. The correlation functions are calculated using Eqs. 48 and 52, for a point source ($\sigma = \mu = 0$). For the model calculations, the observing wavelength is $\lambda = 2\pi/k = 10$ cm. The scattering material lies at a distance D = 320 pc, and the source lies an equal distance beyond the screen, at R = 320 pc. The standard deviation of the angular broadening is $\theta = 2$ mas. The temporal smearing is $\tau_0 = 30~\mu \text{sec}$.